Itinerant f-Electron Systems

Börje Johansson

Condensed Matter Theory Group, Physics Department,

Uppsala University, Box 530, Uppsala, Sweden

and

Hans L. Skriver

Center for Atomic-scale Materials Physics and Department of Physics,

Technical University of Denmark, DK-2800 Lyngby, Denmark

Abstract

The electronic structures of the earlier lanthanide and actinide elements are considered, and especially cohesive properties and crystal structures are used to demonstrate the deep involvement of the f electrons in the metallic bonding. The recent observation for samarium of a bct structure at a pressure of about 1 Mbar suggests that the $4f$ electrons at these conditions have become itinerant, and, in addition, the observed axial ratio (c/a) is only reproduced from a calculation with a *ferromagnetic* ordering of the itinerant (metallic) $4f$ electrons. As a consequence of this interpretation of the observed data, a thorough experimental investigation of the crystal structure behaviour of the lanthanides in the megabar pressure range, in particular for the elements Nd-Tb, should be very fruitful. For the earlier actinide elements the ground state crystal structures have recently been obtained theoretically and shown to originate from itinerant $5f$ electrons. Thus, for the first time, the crystal structure of Pu has been derived from basic electronic structure calculations. This firmly establishes that there is a profound change in the behaviour of the $5f$ electrons when proceeding from Pu to the next element Am. Recent theoretical work on the pressure-temperature phase diagram of cerium, where the Mott transition picture of the γ–α transformation is extended to finite temperatures, is reviewed. The high pressure phase of praseodymium is also discussed in terms of itinerant $4f$ electrons. This picture fits nicely with the behaviour of highly compressed samarium metal mentioned above. Accordingly, the normally localized $4f$ electrons can be transformed into a radically new electronic configuration by high pressure.

1 Introduction

Since the present symposium is devoted to metallic magnetism it might seem fairly inappropriate to discuss systems with itinerant f electrons, since most of these systems do not order magnetically. Nevertheless, at the planning stage of the conference program, Allan Mackintosh assured us that this topic was central to the

meeting and that no excuses for the subject were necessary. It remains true that the expectations of finding magnetism in these systems are so high, that its very absence creates a special need for an understanding of the underlying reasons for this unexpected behaviour. In the present contribution we will however limit ourselves to some recent developments where we have been involved, but also restrict ourselves to the behaviour of the condensed phase of some pure elements of particular interest. In doing this, we will pay particular attention to the actual crystal structure adopted by the atoms in the solid. We demonstrate that the crystal structure provides us with important data for formulating a deeper understanding of these systems. We also refer to some review articles where a more complete account of the lanthanide and actinide electronic structure has been given (Johansson and Brooks, 1993; Brooks et al., 1984). In another review article by Brooks and Johansson (1993) the magnetic effects are especially stressed. Despite the rather general absence of magnetism in itinerant f systems, the theoretical studies of samarium at high pressure suggest that *a completely new research field of itinerant magnetism* has been discovered, namely lanthanides at a pressure of 1 Mbar.

The electronic structure determines the ground state crystalline atomic arrangement. Consequently, the experimentally observed crystal structures contain important information about the basic nature of the corresponding electronic configuration. This is especially so when one deals with a system displaying an unique crystal structure, not observed for any other system. This is certainly the case for the α-Pu phase, which has 16 atoms per unit cell. In those particular cases where in addition there is also a crystal structure change observed as a function of volume, one is provided with even more detailed facts that have to be matched by theory. This is one of the reasons why high pressure experiments are particularly useful to monitor the accuracy of the theoretical treatment. It so happens that for the $4f$ and $5f$ elements there are a number of crystal structure transformations which take place both as a function of pressure or as a function of alloying. These circumstances provide further input to an accurate study of the lanthanides and the actinides, but have not yet been fully exploited.

There is also another circumstance that makes investigations of the rare-earth systems particularly challenging for theory. Namely that for some systems under compression, most dramatic electronic phase changes might take place, being accompanied by colossal volume collapses when compared to normal crystalline phase transitions in metallic systems. These changes involve the nature of the $4f$ electrons and their transformation between on the one hand localized non-bonding magnetic moments and on the other hand strong metal bonds. This is an example of a Mott transition between an insulating state and a metallic state within the $4f$ shell, a phase transformation that takes place in the presence of a conduction band built up from s, p, and d orbitals occupied by approximately three electrons. The

most well-known example of this is of course the γ–α transition in cerium. The particular significance of the volume collapse in cerium is due to the fact that the transformation does not involve a change of the crystallographic structure, i.e. the crystal structure is fcc on both sides of the transition.

2 Atomic volume

In Fig. 1 we show the atomic volumes of most of the metals in the Periodic Table. The most obvious feature is the similarity between the d transition elements, in particular between the $4d$ and $5d$ metals. Also the volume of the $3d$ elements display an essentially parabolic variation, although there are clear deviations for Mn, Fe and Co, a fact which can be assigned to their magnetic properties. The parabolic behaviour originates from the metallic bonding of the d electrons, where for the earlier elements of the d transition series the bonding part of the d band is being occupied and for the heavier elements the anti-bonding part of the d band is becoming filled. This regularity among the d elements is quite well understood today and indeed electronic structure calculations, utilizing the local density approximation for the exchange and correlation energy, have been very successfully applied to these elements during the last ten years or so. This theory can easily be extended so that magnetism can be treated as well. Thereby the anomalous volumes of the magnetic $3d$ elements can be explained as a consequence of the magnetization, which removes part of the original metallic bonding. This loss of bonding is partly compensated by a corresponding gain in exchange energy due to polarization of the electron spins.

A most interesting feature in Fig. 1 is the behaviour of the lanthanides. As can be seen there is only a very small volume contraction as one proceeds through the series. The similarity between the individual elements is explained as due to the fact that all the elements have three valence electrons, starting and ending with the two obvious cases lanthanum and lutetium having zero and fourteen $4f$ electrons, respectively, and therefore three valence electrons filling the conduction band formed from $6s$, $6p$ and $5d$ orbitals. The two elements Eu and Yb have only two valence electrons and therefore their equilibrium volumes are distinctly higher than for the other trivalent lanthanides. Another point to notice is that the atomic volume for cerium in the α-phase deviates considerably from the general behaviour of the lanthanide elements. Later we will show that this is due to itinerant $4f$ electrons, a property which is in contrast to all the other lanthanides where the $4f$ electrons are localized with an integral occupation of the atomic-like f level, $4f^n$.

Turning now to the actinide series a most interesting and challenging behaviour can easily be distinguished. In the beginning of the series we notice once more a

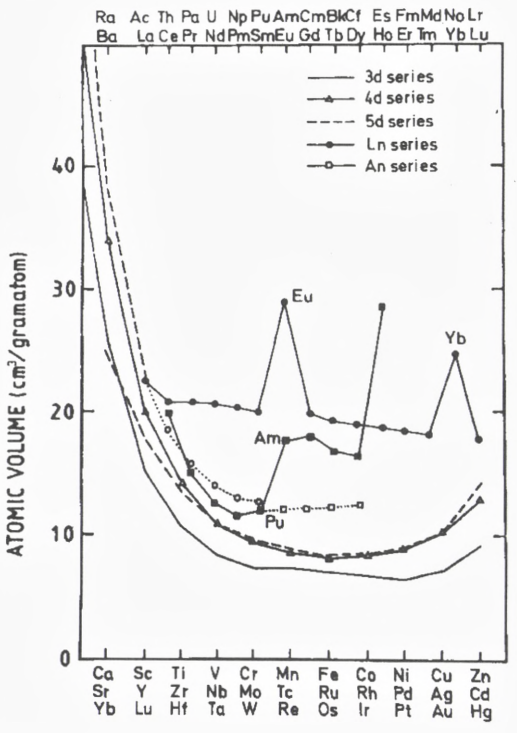

Figure 1. The experimental equilibrium atomic volumes of the $3d$, $4d$ and $5d$ transition metals, the lanthanides and the actinides. The low volume data for the earlier lanthanides and the transplutonium elements are estimations of the equilibrium volumes for the case that the f electrons were itinerant (and paramagnetic).

parabolic decrease of the atomic volume as a function of the atomic number. Then suddenly, between Pu and Am, there is a dramatic change and the volume increases by about 50%. Thus, a drastic transformation of the electronic structure must take place between Pu and Am. This difference has been explained as a transition from metallic to insulating $5f$ electron behaviour and a good account of the volumes for the earlier actinides as well as the volume jump between Pu and Am has already been obtained in the work by Skriver et al. (1978 and 1980).

From Am and onwards the atomic volumes behave very similar to the lanthanides. It is only when we arrive at Es that there is another distinct difference between the lanthanides and actinides, since the deviating Es volume is not observed for the corresponding $4f$ element, Ho. The reason is that several of the late actinide elements will be divalent in the metal phase (Johansson, 1978) in contrast to the heavy lanthanides where only Yb is found to be divalent in the

metallic state. We also notice from Fig. 1 that Am is trivalent, in clear contrast to its corresponding element among the lanthanides, Eu, which is divalent. This difference is well understood and has led to the prediction of superconductivity in Am (Johansson and Rosengren, 1975a), which later was confirmed experimentally (Smith and Haire, 1978).

Once more we emphasize that at zero pressure there is a profound difference between the early and late actinide metals, in the sense that the $5f$ electrons are itinerant (metallic) for the elements up to and including Pu, while they are localized and non-bonding (atomic-like) for the elements beyond Pu (Johansson, 1975). Thus in this respect the later (heavier) actinides and their $5f$ electrons behave like most of the lanthanides with their localized $4f^n$ atomic-like configurations. On the other hand, among the lanthanides the first element with a substantial occupation of the $4f$ shell, i.e. cerium, shows already at rather low pressures or at low temperatures a behaviour very reminiscent of the early actinides (Johansson, 1974). Thus for the actinides there are five elements (Th-Pu) showing itinerant $5f$ behaviour before localization sets in when the atomic number is increased from Pu to Am, while for the lanthanides only one element exhibits $4f$ itinerant properties, i.e. cerium, and thereafter localization is energetically favoured for all the heavier $4f$ elements. We illustrate this by arranging the actinides relative to the lanthanides introducing a displacement in atomic number (Johansson and Rosengren, 1975a):

				Ce	Pr	Nd	Pm	Sm	Eu	Gd
Th	Pa	U	Np	Pu	Am	Cm	Bk	Cf	Es	Fm

(The physical reason for this displacement is the larger spatial extent of the $5f$ orbital as compared to the $4f$ orbital for the corresponding element.) This suggests a most interesting connection between the $4f$ and $5f$ series, but this has not yet been fully explored.

Further evidence of the validity of this picture comes from the fact that the element following cerium, i.e. praseodymium, shows a volume collapse (Smith and Akella, 1982; Grosshans et al., 1983) of about 10% at 200 kbar and that this dense phase shows similarities with the early actinides. Thus application of a moderate pressure moves the division line between itinerant and localized $4f$ behaviour one atomic number upwards so that now, at these new external conditions (i.e. a pressure of about 220 kbar or so), two lanthanide elements show correspondence to the early actinides. The important conclusion is that depending on the external pressure, more than one element of the lanthanides can be brought into a state with close similarities to the early actinides. This relationship between the two f series was pointed out more than twenty years ago and a generalized phase diagram for the actinides was constructed (Johansson 1974) and compared with the individ-

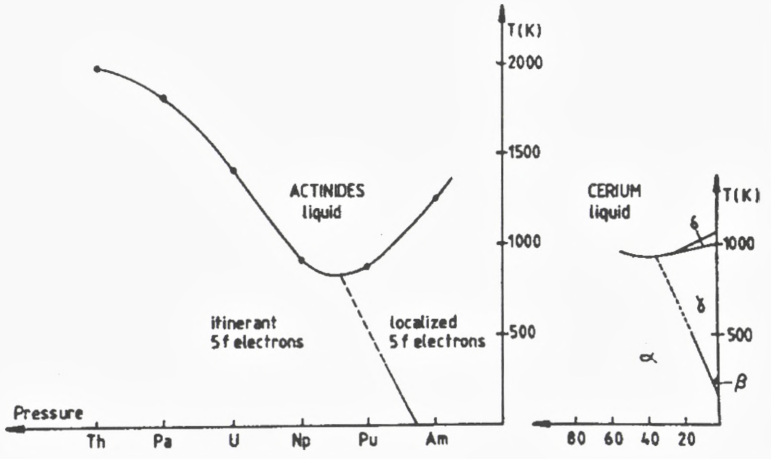

Figure 2. Melting temperatures for the actinide elements (left) and the $P-T$ phase diagram for cerium (right) (Johansson, 1974). The effect of pressure on an individual element is to make it behave more similarly to its predecessor in the series. This is schematically indicated by a tentative pressure axis on the left. The indicated transition line for the transition between localized and itinerant $5f$ behaviour (Mott transition) as a function of atomic number Z (or pressure for an individual element) has been included schematically. Its extension to the minimum point of the melting curve has been drawn as a suggestive analogy to the behaviour in cerium metal. Also, in the $P-T$ phase diagram for cerium an extension of the γ–α transition line to the minimum of the melting temperature is indicated by a dashed line.

ual pressure-temperature phase diagram for cerium metal (Fig. 2). This diagram for the actinides was later developed further by Kmetko and Smith (1983), who constructed a generalized phase diagram for actinide alloy systems, i.e. for alloys between actinide metals.

3 Crystal structure for itinerant f-electron systems

Turning to the complex structures associated with the itinerant f electrons, there has very recently been some substantial progress in the theoretical understanding. Wills and Eriksson (1992) showed that the ground state crystal structure for Pa is the bct phase, in good agreement with the data available at ambient conditions. For the next element, U, they indeed obtained that α-U is the most stable phase, as required from experiments. However, it is interesting to notice that at high pressures the high symmetry bcc structure is found to become sta-

ble. Söderlind et al. (1994a, 1995a) investigated the Np metal in two papers, the first of which utilized the LDA approximation to the exchange-correlation energy functional, and the second of which applied the more involved GGA approximation. In Fig. 3 we show the energy versus volume diagram for Np obtained by Söderlind et al. (1995a). As can be noticed, the α-Np phase is calculated to be the most stable crystal structure at equilibrium and for small pressures. At high pres-

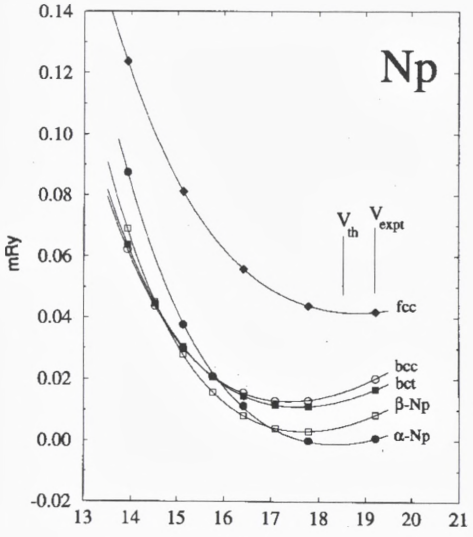

Figure 3. Calculated total energies as a function of volume for the α-Np, β-Np, α-U, bct, bcc, hcp, and fcc crystals of neptunium metal. The points represent calculated values and the solid lines connecting them show the Murnaghan functions as obtained by a least-square fit to the calculated energies.

sures, we again find that the bcc structure is the most stable form. Just recently Söderlind et al. (1997) completed a similar study for Pu metal, where the observed low temperature phase is a monoclinic phase with a wide range of different nearest neighbour distances and as many as 16 atoms per unit cell. Also here the computed theoretical data agree well with known experimental data. Again the bcc structure is found to be the most stable structure at high pressure conditions (Fig. 4). This agreement concerning the equilibrium crystal structure is most satisfactory in view of the complexity of the structure of the plutonium metal. This shows that full-potential electronic structure methods combined with an appropriate density functional treatment of the electron–electron interaction are capable of treating

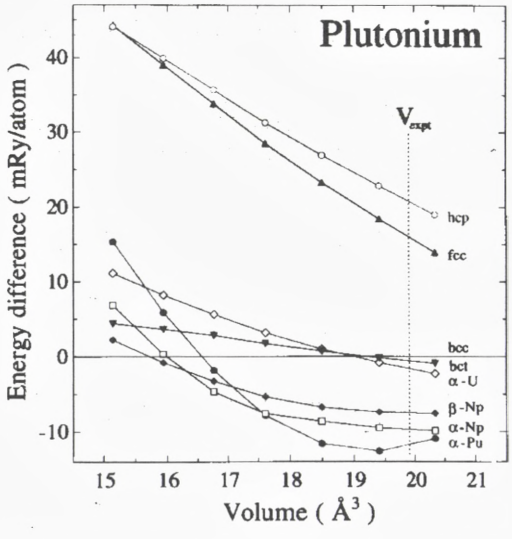

Figure 4. Total energy for plutonium, calculated in the α-Pu, α-Np, β-Np, α-U, bct ($c/a = 0.85$), hcp (ideal c/a), and fcc crystal structures, relative to the bcc structure, as a function of volume.

as heavy elements as the actinides with the same accuracy as for the d transition elements. With this achievement one may conclude that theory has demonstrated its wide versatility as regards the electronic structure of the metallic Elements.

Söderlind et al. (1995a) also analyzed their results in terms of a canonical treatment of the f states and the crystal structure stabilities as a function of f band filling. Such a comparison is only meaningful between the fcc, hcp and bcc structures which have almost identical Madelung energies. This comparison is reproduced in Fig. 5. One notices in particular the strong preference of the bcc structure for the elements beyond uranium. However, this structure is not observed experimentally for volumes close to equilibrium conditions. Instead heavy displacements of the atoms distort the bcc structure into low symmetry phases. This is possible energetically since the states driving these distortions are the narrow f bands close to the Fermi energy. For compressed volumes the f bandwidth will have increased to such an extent that distortions are no longer energetically favoured. From the behaviour of the canonical one-electron energy sums it is obvious that the bcc structure should be the favoured one at these wide-band conditions. Nevertheless, and unfortunately, at present it seems very difficult to produce a theoretical explanation for the occurrence of the actinide structures with the same simplicity as is found for the d transition elements. However, one may still clam that a big step in this direction has been taken for the actinides. Namely, that the equilib-

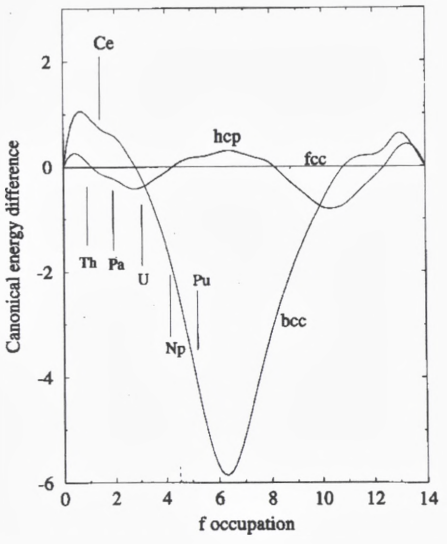

Figure 5. Canonical f band structural energy differences (arbitrary units) as a function of f band occupation. The fcc canonical energy defines the zero energy level of the plot. Calculated equilibrium f band occupations for the light actinides (Th-Pu) are also shown as vertical lines.

rium volume structures can be considered as based upon the bcc structure, which undergoes a substantial distortion due to the narrow f band states. Söderlind et al. (1995b) also performed an interesting study of two d transition metals and one simple metal, which is highly relevant to the present discussion. They expanded the Fe, Nb, and Al metals, and investigated the structure stability as a function of expansion. The most interesting observation was that for all three of these metals, the α-U structure becomes favoured relative to the structure observed at normal conditions. Thus, again the very fact that the dominant bonding states narrow their energy bandwidth upon expansion makes it energetically favourable to undergo distortions away from high symmetry structures. Therefore it is not primarily the f orbital character that determines the crystal structure, but rather the bandwidth of the bonding orbitals is of decisive importance for a distorted metal. The canonical structure sequences as a function of band-filling are however different between for example d and f bands. The difficulty in finding a simple theory for distorted structures depends on the large difference between the Madelung energies for the different structures. For the d transition metals, where, based on experimental data, one may allow oneself to restrict the comparison to the three main metal crystal structures – bcc, hcp, and fcc – one can to a good accuracy neglect the difference between the Madelung sums for the three structures, thereby

gaining enormously in simplicity. Nevertheless, as regards the crystalline forms of the metal elements, we believe that a great step forward has been taken towards a general capability to handle the basic interactions giving rise to the wide range of crystal structures observed among the elements. The fact that we can treat the $5f$ elements and the d elements equally well means that today we essentially cover the whole Periodic Table, and as regards crystal structure studies we see no particular limitation of the present local density approximation.

In this context it is also of interest to consider thorium metal. For a long time the observed fcc crystal structure was taken as evidence for a normal transition metal behaviour dominated by the d electron character. However it was recently shown (Ahuja et al., 1995) that this is not at all the case, since instead a regular tetravalent d transition metal should either have an hcp, bcc or ω-structure. It was only when the presence of some $5f$ character in the conduction band was included in the theoretical treatment that the observed fcc structure could be reproduced. Therefore, actually all the metals Th-Pu can be said to have anomalous crystal structures when compared to the rest of the periodic system. It is most important to notice that these structures can only be explained by the bonding properties of the itinerant $5f$ electrons. Thus, the recent theoretical work regarding the actinide crystal structures has shown that the earlier theory regarding the cohesion of these metals is correct, namely that the lighter elements form a unique series of metals with $5f$ electrons as the dominant part of the metallic bonding and that the heavier elements behave as a second rare-earth series with atomic-like $5f$ electrons (Johansson, 1975; Johansson and Rosengren, 1975b).

4 Local-moment collapse in compressed Sm metal

Recent developments of the experimental high pressure technique have made it possible to study materials at static pressures in the Megabar range (Mao et al., 1989; Vohra and Ruoff, 1990). One can now begin to investigate solids under new experimental conditions, where the volume is reduced to typically half of its normal value ($V/V_0 = 0.5$, where V_0 is the equilibrium volume). It has therefore become a great challenge for theory to cover this new physical regime for various classes of materials.

The magnetic rare-earth metals are especially interesting in connection with extreme compressions. Normally, in most cases the $4f$ electrons are localized and the associated magnetic moments are very well described by atomic theory (Jensen and Mackintosh, 1991). This fact forms the basis for the so-called standard model for rare-earth systems. Furthermore, the lanthanides are well understood from a trivalent picture (Ce, Eu, and Yb are exceptions) and the metallic bond originates

from a rather broad conduction band containing three (*spd*) electrons. The trivalent metals crystallize in hexagonal close packed structures (hcp, Sm-type, and dhcp). Theoretical calculations (Duthie and Pettifor, 1977; Skriver, 1985) show that the crystal structure sequence is correlated with the d occupation of the valence band [or to a related quantity, the ratio between the metallic and ionic radii (Johansson and Rosengren, 1975a)]. It has actually been demonstrated that the crystal structure sequence found when traversing the lanthanide series, dhcp $\rightarrow$ Sm-type $\rightarrow$ hcp, originates from the decreasing d occupation. Also, applying pressure to a late lanthanide metal increases the d character of the metallic bond and correspondingly the reversed structure sequence, hcp $\rightarrow$ Sm-type $\rightarrow$ dhcp, is observed. At sufficiently high pressure the trivalent lanthanide metals transform first to the fcc structure and then to a trigonal distortion of the fcc structure (Vohra et al., 1991; Staun-Olsen et al., 1991; Grosshans and Holzapfel, 1992). Hence, all previous high pressure work show transitions between close packed structures, and the understanding of this behaviour is based on a trivalent ground state with chemically inert $4f$ electrons (Johansson and Rosengren, 1975). However, relatively recent experimental high pressure work (Vohra et al., 1991) showed that at around 1 Mbar Sm adopts a quite unique body centered tetragonal (bct) structure. Such kind of structures (open, low symmetric) have previously mainly been found in delocalized f metals and in the present context it is tempting to associate the bct structure with an onset of f bonding (Johansson, 1974).

With this in mind Söderlind et al. (1993) performed a study of Sm at these new extreme conditions. In order to determine when the $4f$ states might become itinerant in Sm, these authors compared the bonding energy associated with delocalized f states with the atomic polarization energy (E(pol)) associated with localized f states. To do this they had to compare the total energy between two different electronic states for highly compressed samarium, namely the standard localized $4f^5(^6G_{\frac{5}{2}})$ trivalent metallic state and the itinerant $4f$ state, where for the latter not only the *spd* states but also the f states are part of the conduction band. The total energies for the two phases were calculated using a full potential linear method (FPLMTO) (Wills and Cooper, 1987). These calculations make no shape approximation for the charge density and potential and are based on the local density approximation of the density functional theory. For the localized phase the $4f$ states were treated as part of the core and with a statistical occupation of the $4f_{\frac{5}{2}}$ and $4f_{\frac{7}{2}}$ levels, which corresponds to the grand barycentre for the atomic-like $4f^5$ manifold.The total energies for the two phases will therefore be directly comparable if the energy difference between the grand barycentre and the lowest atomic multiplet is taken into account for the trivalent state (Johansson et al., 1980; Johansson and Skriver, 1982). This energy, E(pol), is known to be 5.8 eV from analysis of atomic spectra (Nugent, 1970).

At zero pressure the crystal structure of samarium metal is a 9 layer stacking sequence of hexagonal planes (Sm-structure) and the experimental equilibrium atomic volume V_0 is equal to 33.2 Å^3. However, as mentioned above it is well-known that the lighter lanthanides under high pressure transform into the fcc structure (Vohra et al., 1991). Therefore Söderlind et al. (1993) used the fcc structure in the calculations for the standard local moment, trivalent samarium metal and for the itinerant state they used the experimentally reported high pressure structure, bct (with the observed axial ratio $c/a = 1.76$). For the study of the local moment collapse these particular choices of structures are however not crucial.

By introducing the atomic energy, E(pol), Söderlind et al. (1993) could perform a proper energy comparison between the localized and itinerant states from first principles calculations of the total energies as a function of volume (Johansson and Skriver, 1982). This comparison is shown in Fig. 6, where the total energy has been plotted as a function of volume both for the delocalized and localized phases. Notice that there is a transition from the localized fcc phase at 18.3 Å^3

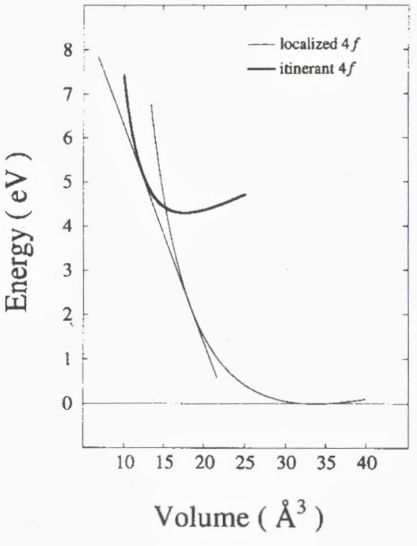

Figure 6. Total energies for Sm with localized (thin line) and delocalized (thick line) $4f$ electrons. The energy for the localized phase is corrected by the polarization energy E(pol) in order to account for the lowest multiplet state of the $4f^5$ configuration (see text). The transition pressure is obtained from the common tangent construction.

to the delocalized bct phase. The transition pressure, obtained from the common tangent shown in Fig. 1, is 0.8 Mbar. This result is consistent with the experimental finding of a bct structure being stable at high compressions, since it is known that chemically bonding f electrons favour open, low symmetry structures (Johansson, 1974). However, experimentally the volume collapse associated with the bct phase is much smaller than the calculated value, a point we will return to below.

The validity of the finding that the highly compressed phase of Sm has delocalized $4f$ states, can be further investigated by consideration of the crystallographic parameters, like for example the c/a axis ratio of the bct structure. This is in fact a very sensitive test, since crystal structure energy differences are very small and sensitive to the details of the electronic structure. Söderlind et al. (1993) treated the $4f$ states as delocalized and calculated the total energies of Sm using three different crystal structures; fcc, bct, and the orthorhombic α-U structure. The α-U structure was included since this structure is found in many delocalized f electron systems [U (Zachariasen, 1952); Ce (Ellinger and Zachariasen, 1974); Pr (Smith and Akella, 1982; Grosshans et al., 1983) and Am (Benedict, 1984)]. This was done at volumes where it is known experimentally that the bct structure is stable, with a c/a ratio of 1.76. For the α-U structure the crystallographic parameters corresponding to α-Ce were used. These calculations covered the volume range $0.3 < V/V_0 < 0.4$. It was found that the bct structure is favoured over the α-U structure (by about 4–8 mRy/atom) as well as over the fcc structure (by 10–30 mRy/atom). It was due to the presence of itinerant f states in the theoretical treatment that the bct structure obtained the lowest energy.

To further illustrate the importance of the f electrons for the crystal structure Söderlind et al. (1993) calculated the energy of the Bain path (total energy as a function of the c/a ratio for the bct structure) for both delocalized and trivalent Sm at a compression $V/V_0 = 0.37$ (Fig. 7). It is worthwhile to remark here that the bct structure is the same as the bcc structure for $c/a = 1$ and the same as the fcc structure for $c/a = \sqrt{2}$. Fig. 7 shows that for the trivalent localized $4f$ configuration the bcc structure is stable, in disagreement with the experimental finding. However, the delocalized (paramagnetic) configuration yields the correct structure, bct. Hence, only for delocalized states could Söderlind et al. (1993) reproduce the correct structure. However, the calculated c/a ratio (1.95) is substantially larger than the experimental data (1.76). This large disagreement indicates that the $4f$ contribution to the bonding is overemphasized. However, in these calculations a paramagnetic state was imposed. Removing this restriction and allowing the system to break the spin degeneracy, a very substantial spin moment was obtained, which is displayed in Fig. 8 as a function of volume for the ferromagnetic state. Notice that at volumes where one finds the delocalized phase to be stable (see Fig. 6) the magnetic moment is changing quite dramatically as a function of volume.

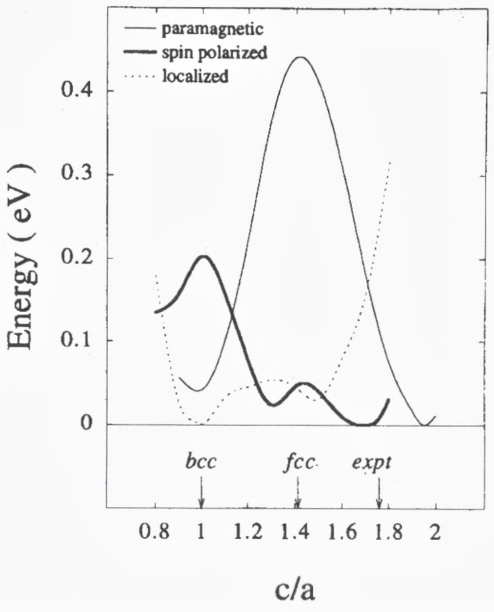

Figure 7. Theoretical Bain path for Sm at 37 % of the experimental volume. The thin full-drawn and bold full-drawn lines refer to a treatment of the $4f$ electrons as itinerant-paramagnetic and itinerant-spin polarized, respectively. The dotted line represents the result for the localized phase, where the $4f$ electrons are considered as part of the inert core.

Nevertheless, at the transition volume the spin moment is substantial, about 4 μ_B. An account of this ferromagnetic state in the theoretical equation-of-state would decrease most significantly the volume collapse ascribed to the delocalization process (compare above). At sufficiently low volumes the moment disappears and Sm metal becomes a $4f$ delocalized paramagnet. Söderlind et al. (1993) also calculated the energy of the Bain path for the ferromagnetic phase of Sm (Fig. 7). Notice that now, for the spin polarized state, the theoretical c/a ratio (1.70) agrees very well with experimental data. Therefore, both direct total energy considerations as well as the more indirect details concerning the atomic structural arrangement suggest that Sm metal at high pressures is a $4f$ itinerant magnet.

Based on the above comparisons with experimental data, it is clear that strong theoretical evidence has been obtained for that the localized $4f$ moment in samarium metal has become itinerant in the Mbar pressure range. This is remarkable since the samarium $4f^5$ moment is normally considered to be extremely stable against external influences. This finding opens the prospects that even the local moments in europium, gadolinium and terbium might become unstable at pressures

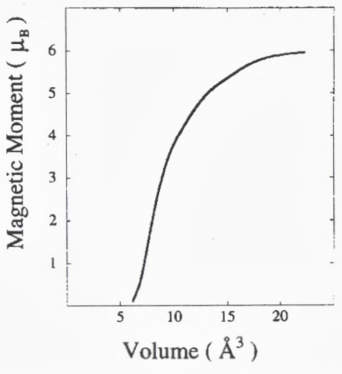

Figure 8. The calculated ferromagnetic spin moment for the itinerant phase of Sm as a function of volume, i.e. the $4f$ electrons are considered as conduction electrons.

attainable at laboratory conditions. The discovery of ferromagnetism in samarium at high compressions strongly suggests that we might have disclosed a *new research area for itinerant magnetism*, namely lanthanides at a pressure of 1 Mbar.

5 Calculated phase diagram for Ce metal

Cerium is one of the most fascinating elements in the Periodic Table. It has, in particular, an extremely rich phase diagram with at least five allotropic forms (Koskenmaki and Gschneidner, 1979). Most attention has been focussed on the γ–α isostructural phase-transition where the high-volume face-centered cubic (fcc) γ phase collapses into the low-volume fcc α-phase at a pressure of about 7 kbar. There is little doubt about the electronic nature of this transition and a great number of theoretical investigations have dealt with the electronic properties of cerium (Coqblin and Blandin, 1968; Ramirez and Falicov, 1971; Hirst, 1974; Johansson, 1974; Glötzel, 1978; Podloucky and Glötzel, 1983; Pickett et al., 1981; Min et al., 1986; Allen and Martin, 1982; Lavagna et al., 1982, 1983; Gunnarsson and Schönhammer, 1983; Liu et al., 1992; Allen and Liu, 1992; Eriksson et al., 1990; Szotek et al., 1994; Svane, 1994).

The unusual behaviour of Ce has been described within a number of models that may be classified into three groups. However, here we will only consider the Mott transition picture advocated by one of the authors (Johansson, 1974). According to this model the nature of the $4f$ states in Ce changes from local non-bonding in the γ-phase to itinerant bonding in the α-phase. A number of recent ab initio calculations, where one assumes that the $4f$ electron is localized in γ-Ce but delocalized in α- and α'-Ce, have given excellent results for the ground state

properties of γ- and α-Ce (Eriksson et al., 1990; Szotek et al., 1994; Svane, 1994) as well as for the α'-phase (Wills et al.,1991; Eriksson et al., 1992). Moreover, by applying the self-interaction corrected (SIC) local density approximation (LDA) Szotek et al. (1994) and Svane (1994) found that in spite of the dramatic change in the electronic structure at the transition, the difference in total energy between γ- and α-Ce is of the order of mRy. A similar energy difference was found by Eriksson et al. (1990) and this is exactly what is required to describe the transition in the Mott transition model.

Recently the pressure-temperature phase diagram of cerium was calculated by Johansson et al. (1995) based on the Mott transition picture and the thermodynamic

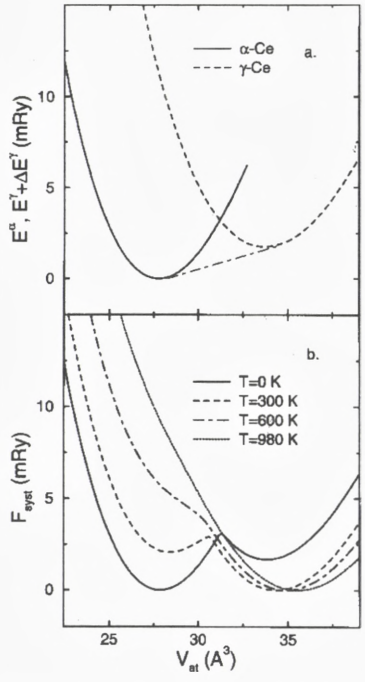

Figure 9. Binding energy curves for α- and γ-Ce (a) and the free energy of the system $F_{\rm syst}$ at different temperatures (b) as a function of atomic volume V_{at}. The energies in (a) are relative to the minimum energy for α-Ce while in (b) they are relative to the minimum value of $F_{\rm syst}$ at the corresponding temperature. The dot-dashed line in (a) corresponds to the extrapolated experimental value of -6 kbar for the (negative) transition pressure at zero temperature. The energy shift ΔE in Eq. (5) has been adjusted to reproduce this transition pressure.

model illustrated in Fig. 9. According to this, there are at zero temperature two phases for Ce, a low volume α-phase which is stable, and a high volume γ-phase which is metastable. The resulting binding energy curve viewed as a function of volume is formed by two branches corresponding to α- and γ-Ce, respectively, which cross at some intermediate volume. The transition between α- and γ-Ce represented by the common tangent in Fig. 1 occurs when the lattice is expanded and from the experimental data reviewed by Koskenmaki and Gschneidner (1979) the transition pressure is deduced to be -6 kbar.

As the temperature increases the state (α or γ) which is metastable may be thermally populated. Hence, there is a probability x of finding a γ-Ce atom in the system and a $1-x$ probability of finding an α-Ce atom. Therefore, one may consider the cerium metal as a pseudo-alloy between the γ- and α-phases and write its free energy F_{alloy} for any "concentration" x, volume V and temperature T as

$$F_{\text{alloy}}(x,V,T) = E(x,V) - TS(x) + F_{lv}(x,V,T). \tag{1}$$

Here, E is an average internal energy per atom in the pseudo-alloy at $T=0$, S the entropy, and F_{lv} the free energy of the lattice vibrations.

The configurational mixing entropy is taken into account by using the mean-field (MF) approximation

$$S_{\text{conf}}(x) = -k_B[x\ln x + (1-x)\ln(1-x)], \tag{2}$$

where k_B is the Boltzmann constant. In addition to this also the magnetic entropy from the localized magnetic moment on the γ-Ce atoms must be included. Assuming that for temperatures of interest only the ground state multiplet with total angular momentum $J = \frac{5}{2}$ is appreciably populated, the magnetic entropy becomes

$$S_{\text{magn}}(x) = k_B x \ln(2J+1). \tag{3}$$

Finally, the vibrational free energy $F_{lv}(x,V,T)$ is estimated from the Debye-Grüneisen model (Moruzzi et al.,1988).

Since γ-cerium can transfer into α-cerium and vice versa, the alloy concentration is not a free parameter as in the case of a real alloy system. Instead, the concentration x_{eq} is determined from the value which for a fixed volume and temperature minimizes the free energy. Hence, one arrives at the final expression for the free energy of the system

$$F_{\text{syst}}(V,T) = F_{\text{alloy}}(x_{eq}(V,T),V,T). \tag{4}$$

Having derived F_{syst} as a function of volume one may obtain Gibbs free energy $G = F + PV$, where P is the pressure, and determine the transition pressure of

the γ–α phase change at any temperature. In this way the P–T phase diagram for Ce can be obtained, based on the Mott transition model for the electronic transformation within the $4f$ shell.

To obtain realistic results, a good description is needed for the initial α- and γ-states as well as for the alloy total energy $E(x, V)$. In particular, for the accuracy of the calculated phase diagram it is important that the equilibrium volumes of pure γ- and α-Ce are well reproduced by the total energy calculations. For this purpose Johansson et al. (1995) used the scalar-relativistic linear muffin-tin orbitals (LMTO) method, within the atomic sphere approximation (ASA) and in the tight-binding representation (Andersen et al., 1985; Gunnarsson et al., 1983; Skriver, 1984). This was performed in conjunction with a Green's function technique and a treatment of the alloy utilizing a scheme based on the single-site coherent-potential approximation (SS-CPA) (Johnson et al., 1990; Abrikosov et al., 1993).

To describe paramagnetic α-Ce the $4f$-electron is regarded as a delocalized valence electron. Note that such an assumption together with LDA is known to lead to an underestimate of the equilibrium volume and an overestimate of the bulk modulus compared with the experimental values. However, this is basically an effect of using the LDA rather than an effect associated with any special properties of α-Ce. Moreover, Söderlind et al. (1994) found that the ground state parameters α-Ce are very sensitive to the approximation used for the exchange-correlation functional. When one applies the Becke–Perdew gradient correction (GGA, Perdew, 1986; Becke, 1988) to the exchange-correlation potential one obtains a much better agreement between the calculated and experimental atomic volume and bulk modulus for α-Ce. For this reason, Johansson et al. (1995) chose to describe pure α-Ce and the α-Ce atoms in the alloy within this approximation for exchange and correlation.

The localized $4f$-electron in γ-Ce can be accounted for by means of the SIC-LDA scheme (Szotek et al., 1994; Svane, 1994). However, in an alloy this becomes numerically very complicated and instead an approach used earlier by Min et al. (1986), can be applied. In this scheme the $4f$-electron in γ-Ce is treated as fully localized by including it as part of the inert core, but the f functions are kept in the LMTO valence basis set. Using the Vosko–Wilk–Nusair parametrization (Vosko et al., 1980) of the exchange-correlation energy density and potential the calculations for the equilibrium atomic volume and bulk modulus of γ-Ce show excellent agreement with the results obtained from the SIC-LDA calculations (Szotek et al., 1994; Svane, 1994) as well as with experimental values. These are the set of approximations which Johansson et al. (1995) applied in the description of the pseudo-alloy.

Within the frozen core approximation (Gunnarsson et al., 1983), used in the simplified description of γ-Ce, the contribution to the energy from the localized

$4f$ electron is discarded. The energies of the two phases of Ce must therefore be aligned by an energy shift ΔE added, for instance, to the total energy of γ-Ce. This is the only adjustable parameter in the model and it is only introduced for technical reasons rather than as a matter of principles. The internal energy $E(x, V)$ in Eq. (1) may now be written in the form

$$E(x, V) = (1 - x)E_\alpha(x, V) + xE_\gamma(x, V) + \Delta E, \tag{5}$$

where $E_j(x, V), j = \alpha, \gamma$, is the calculated total energy per α (or γ) atom.

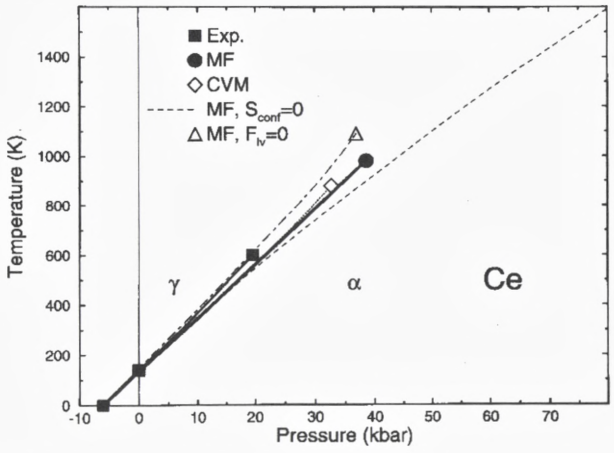

Figure 10. Pseudoequilibrium pressure-temperature phase diagram for Ce. The experimental result is taken from Koskenmaki and Gschneidner (1979) and shown by the full line and filled squares. The zero temperature is obtained by extrapolation. The diagram calculated within the mean-field (MF) approximation and with all the contributions to the free energy included is shown by the heavy line. The corresponding critical point is shown by the full circle. The results obtained by the cluster variation method (CVM) are indicated by the dotted line and the open diamond. The dashed line corresponds to a MF phase diagram where the effect of alloying is neglected, i.e. $S_{\text{conf}} = 0$, and the dot-dashed line with the open triangle corresponds to the MF result calculated without the vibrational contribution to the free energy, i.e. $F_{lv} = 0$.

The calculated phase diagram for the γ–α transition in Ce is shown in Fig. 2 together with the experimental phase diagram taken from Koskenmaki and Gschneidner (1979). It is seen, that the theory, correctly describes the salient features of the phase diagram, i.e., the linear dependence of the transition temperature on pressure and the existence of a critical point. The zero pressure transition tem-

perature is calculated to be 135 K in excellent agreement with the experimental value 141 ± 10 K. The critical point is found at 980 K and 38.6 kbar, in fair agreement with experiment (600 ± 50 K, 19.6 ± 2 kbar) (Koskenmaki and Gschneidner, 1979). A small overestimate of the critical temperature and pressure is to be expected because of the application of the mean-field approximation for the entropy. If the more elaborate cluster variation method (CVM) is used in conjunction with the CPA-Connolly–Williams scheme for calculating interatomic interactions (Abrikosov et al., 1993) an even better result for the calculated P–T diagram is obtained (compare Fig. 10).

An analysis of the results shows that the dominating entropy contribution originates from the magnetic moment on the Ce atoms, which is zero in the α-phase and $k_B \ln(2J+1)$ in the γ-phase. The transition pressure can now easily be estimated as (Johansson et al., 1993)

$$P(T) = P_0 + k_B T (V_{\gamma 0} - V_{\alpha 0})^{-1} \ln(2J+1), \tag{6}$$

where the subscript 0 refers to properties at $T = 0$. This immediately explains the observed linear dependence of the transition temperature on the pressure. Finally, for the artificial, intermediate volumes the equilibrium concentration x_{eq} is substantial already at relatively low temperatures (about 300 K). This results in a *softening* of the crossover between the two branches of the free energy, as shown in Fig. 9b, and in the end to *the occurrence of the critical point.* When the effect of alloying is completely neglected the low temperature behaviour of the phase diagram is almost identical to that of the complete calculation, but the critical point is lost.

References

Abrikosov IA, Ruban AV, Kats DYa and Vekilov YuH, 1993: J. Phys. Condens. Matter **5**, 1271

Ahuja R, Eriksson O, Wills JM and Johansson B, 1995: Phys. Rev. Lett. **75**, 3473

Allen JW and Martin RM, 1982: Phys. Rev. Lett. **49**, 1106

Allen JW and Liu LZ, 1992: Phys. Rev. B **46**, 5047

Andersen OK, Jepsen O and Glötzel D, 1985: in *Highlights of Condensed-Matter Theory*, eds. F. Bassani, F. Fumi and M.P. Tosi (North Holland, New York)

Becke AD, 1988: Phys. Rev. A **38**, 3098

Benedict U, 1984: J. Phys. Colloq. (Paris) **45**, 145

Brooks MSS, Johansson B and Skriver HL, 1984: *Handbook on the Physics and Chemistry of the Actinides*, eds. A.J. Freeman and G.H. Lander (North-Holland, Amsterdam, 1984) p. 153

Brooks MSS and Johansson B, 1993: *Handbook of Magnetic Materials*, ed. K.H.J. Buschow (Elsevier, Amsterdam) Vol. 7, p. 139

Coqblin B and Blandin A, 1968: Adv. Phys. **17**, 281

Duthie JC and Pettifor DG, 1977: Phys. Rev. Lett. **38**, 564

Ellinger FH and Zachariasen WH, 1974: Phys. Rev. Lett. **32**, 773

Eriksson O, Brooks MSS and Johansson B, 1990: Phys. Rev. B **41**, 7311
Eriksson O, Wills JM and Boring AM, 1992: Phys. Rev. B **46**, 12981
Glötzel D, 1978: J. Phys. F **8**, L163
Grosshans WA, Vohra YK and Holzapfel WB, 1983: J. Phys. F **13**, 14
Grosshans WA and Holzapfel WB, 1992: Phys. Rev. B **45**, 5171
Gunnarsson O and Schönhammer K, 1983: Phys. Rev. B **28**, 4315
Gunnarsson O, Jepsen O and Andersson OK, 1983: Phys. Rev. B **27**, 7144
Hirst LL, 1974: J. Phys. Chem. Solids **35**, 1285
Jensen J, and Mackintosh AR, 1991: *Rare Earth Magnetism: Structures and Excitations* (Clarendon Press, Oxford)
Johansson B, 1974: Philos. Mag. **30**, 469
Johansson B, 1975: Phys. Rev. B **11**, 2740
Johansson B, 1978: J. Phys. Chem. Solids **39**, 467
Johansson B and Rosengren A, 1975a: Phys. Rev. B **11**, 2836
Johansson B and Rosengren A, 1975b: Phys. Rev. B **11**, 1367
Johansson B, Skriver HL, Mťensson N, Andersen OK and Glötzel D, 1980: Physica B **102b**, 12
Johansson B and Skriver HL, 1982: J. Magn. Magn. Mater. **29**, 217
Johansson B and Brooks MSS, 1993: *Handbook on the Physics and Chemistry of Rare Earths*, eds. K.A. Gschneidner Jr., L. Eyring, G.H. Lander, and G.R. Choppin (Elsevier Science Publishers, Amsterdam) Vol. 1, p. 149
Johansson B, Abrikosov IA, Aldn M, Ruban AV and Skriver HL, 1995: Phys. Rev. Lett. **74**, 2335
Johnson DD, Nicholson DM, Pinski FJ, Gyorffy BL and Stocks GM, 1990: Phys. Rev. B **41**, 9701
Koskenmaki DC and Gschneidner Jr KA, 1979: *Handbook on the Physics and Chemistry of Rare Earths*, eds. K.A. Gschneidner Jr., and L. Eyring (North-Holland, Amsterdam) Vol. 1, p.337
Lavagna M, Lacroix C and Cyrot M, 1982: Phys. Lett. **90A**, 210
Lavagna M, Lacroix C and Cyrot M, 1983: J. Phys. F **13**, 1007
Liu LZ, Allen JW, Gunnarsson O, Cristensen NE and Andersen OK, 1992: Phys. Rev. B **45**, 8934
Mao HK, Wu Y, Hemley RJ, Chen LC, Shu JF and Finger LW, 1989: Science **246**, 649
Moruzzi VL, Janak JF and Schwarz K, 1988: Phys. Rev. B **37**, 790
Min BI, Jansen HJF, Oguchi T and Freeman AJ, 1986: Phys. Rev. B **34**, 369
Nugent LJ, 1970: J. Inorg. Nucl. Chem. **32**, 3485
Perdew JP, 1986: Phys. Rev. B **33**, 8822
Pickett WE, Freeman AJ and Koelling DD, 1981: Phys. Rev. B **23**, 1266
Podloucky R and Glötzel D, 1983: Phys. Rev. B **27**, 3390
Ramirez R and Falicov LM, 1971: Phys. Rev. B **3**, 2425
Skriver HL, 1984: *The LMTO Method* (Springer-Verlag, Berlin)
Skriver HL, 1985: Phys. Rev. B **31**, 1909
Skriver HL, Johansson B and Andersen OK, 1978: Phys. Rev. Lett. **41**, 42
Skriver HL, Johansson B and Andersen OK, 1980: Phys. Rev. Lett. **44**, 1230
Smith GS and Akella J, 1982: J. Appl. Phys. **53**, 9212
Smith JL and Haire RG, 1978: Science **200**, 535
Smith JL and Kmetko EA, 1983: J. Less. Common Metals **90**, 83
Staun-Olsen J, Steenstrup S, Gerward L, Benedict U, Akella J and Smith G, 1990: High Pressure Research **4**, 366
Svane A, 1994: Phys. Rev. Lett. **72**, 1248
Szotek Z, Temmerman WM and Winter H, 1994: Phys. Rev. Lett. **72**, 1244
Söderlind P, Eriksson O, Wills JM and Johansson B, 1993: Phys. Rev. B **48**, 9212
Söderlind P, Wills JM, Boring AM, Johansson B and Eriksson O, 1994a: J. Phys. Condens. Matter **6**, 6573

Söderlind P, Eriksson O, Johansson B and Wills JM, 1994b: Phys. Rev. B **50**, 7291
Söderlind P, Johansson B and Eriksson O, 1995a: Phys. Rev. B **52**, 1631
Söderlind P, Eriksson O, Johansson B, Wills JM and Boring AM, 1995b: Nature **374**, 524
Sösderlind P, Wills JM, Johansson B and Eriksson O, 1997: Phys. Rev. B (in press)
Vohra YK and Ruoff AL, 1990: Phys. Rev. B **42**, 8651
Vohra Y, Akella J, Weir S and Smith G, 1991: Phys. Lett. A **158**, 89
Vosko SH, Wilk L and Nusair M, 1980: Can. J. Phys. **58**, 1200
Wills JM and Cooper BR, 1987: Phys. Rev. B **36**, 3809
Wills JM, Eriksson O and Boring AM, 1991: Phys. Rev. Lett. **67**, 2215
Wills JM and Eriksson O, 1992: Phys. Rev. B **45**, 13879
Zachariasen WH, 1952: Acta Crystallogr. **5**, 19